# Oxygen-induced surface $(2\times2)p4g$ reconstruction of Rh(001)

Y. G. Shen,* A. Qayyum,† D. J. O'Connor, and B. V. King
*Department of Physics, University of Newcastle, New South Wales 2308, Australia*
(Received 12 January 1998; revised manuscript received 22 May 1998)

The room-temperature oxygen-induced $(2\times2)p4g$ clock reconstruction of Rh(001) has been investigated by low-energy alkali ion scattering, recoiling spectrometry, low-energy electron diffraction (LEED), and three-dimensional classical scattering simulations. The oxygen atoms are confirmed to be in the fourfold hollow sites to produce the glide plane symmetry of the substrate observed in the LEED pattern. Quantitative values for the geometrical parameters were obtained by using a reliability $R$-factor analysis to compare the experimental and simulated azimuthal scans. The lateral clockwise-counterclockwise displacement of the surface rhodium atoms is $\Delta x=0.2\pm0.1$ Å and the oxygen height above the substrate is $\Delta h=0.6\pm0.1$ Å. The driving force for this clock reconstruction is discussed and compared with previous results on the Ni(001)-$(2\times2)p4g$-C surface. [S0163-1829(98)07139-2]

## I. INTRODUCTION

Adsorbate-induced reconstructions on certain surfaces are important concerns in chemical reactions, order-disorder phase transitions, and other surface phenomena. Many studies show that these reconstructing processes may strongly influence the electronic structure, and change many physical chemical, and structural properties of surfaces (for good reviews, see Refs. 1 and 2). In order to obtain a detailed understanding of these properties, knowledge of the geometrical structure of an adsorbate-induced surface is essential. For this reason, much effort has recently been put into the development of surface-sensitive experimental spectroscopes and techniques which provide quantitative surface structural information. This then serves as a starting point for theoretical calculations, and also allows one to look at systematic differences between related adsorbate-induced reconstructed surfaces.

In recent years, adsorption of oxygen on the Rh(001) surface has been investigated using spot-profile analysis low-energy electron diffraction (SPA-LEED),[3–5] scanning tunneling microscopy (STM),[6] and angle-resolved photoemission.[7,8] These investigations have mainly focused on the order-disorder transitions and the valence-band features of the Rh(001)-O system. The SPA-LEED and STM studies showed that the adsorption of oxygen on Rh(001) at room temperature forms three ordered structures: a $p(2\times2)$ phase at 0.25 ML, an intermediate $c(2\times2)$ phase, and a $(2\times2)p4g$ structure at saturation (0.5 ML). For all structures, the O atoms occupy the fourfold hollow sites. In the $(2\times2)p4g$ structure, the substrate additionally reconstructs by rotation and lateral spreading of the four rhodium atoms surrounding the O atom in order to enlarge the site. Thereby the mirror plane symmetries are broken at the adsorption sites, while glide plane symmetry occurs. This produces two perpendicular glide lines along the directions of the missing spots and leads to the experimentally observed systematic extinction of $(0,n+\frac{1}{2})$ and $(n+\frac{1}{2},0)$ LEED spots at normal electron beam incidence. However, detailed structure of this clock rotated surface is unknown. Neither the O height nor the amount of lateral displacement of surface rhodium atoms has been determined yet.

The purpose of this paper is to apply the technique of low-energy alkali ion scattering and recoiling spectrometry to characterize the reconstruction of the Rh(001)-$(2\times2)p4g$-O surface. Ion scattering and recoiling techniques are highly sensitive to surfaces with clock rotated type reconstructions, and are able to produce data which allow quantitative evaluation of the geometrical parameters.[9–12] Computer simulations of the scattering data, based on a three-dimensional (3D) classical scattering binary collision model, were performed. The oxygen adsorption site and the lateral displacement of surface rhodium atoms were determined by using a reliability $(R)$ factor analysis to compare the experimental and simulated azimuthal scans. The driving force for this clock reconstruction is discussed and compared with previous results on the Ni(001)-$(2\times)p4g$-C surface. The Rh(001) surface and the reconstruction model for the Ni(001)-$(2\times2)p4g$-O surface are shown in Figs. 1(a) and 1(b), respectively. The atomic alignments for the shadowing events responsible for the observed shadowing features of the angular scans described in the text are illustrated.

## II. EXPERIMENT

The experiments were carried out in a stainless-steel UHV chamber ($7\times10^{-11}$ mbar base pressure) equipped with an angle-resolved ion scattering spectroscopy (VSW Scientific Instruments Ltd), LEED (VG Scientific Ltd.), and other facilities for surface characterization and gas adsorption.[12] The scattered and recoiled particles were energy analyzed by a hemispherical electrostatic analyzer with multichannel detection (MCD) to provide high count rates. The use of MCD allows data collection with small ion doses, typically at a beam current density of $3\times10^{-9}$ A cm$^{-2}$ for 1 keV $Li^+$ ions and $5\times10^{-8}$ A cm$^{-2}$for 2 keV $Ne^+$ ions used in this study.

The sample is a rhodium crystal (10 mm diam and 2 mm thick) with a polished (001) surface from Commercial Crystal Laboratory. Final crystal cleaning was achieved by repeated cycles of $Ar^+$ ion bombardment (1 keV, 0.6–0.8 $\mu$A)

 

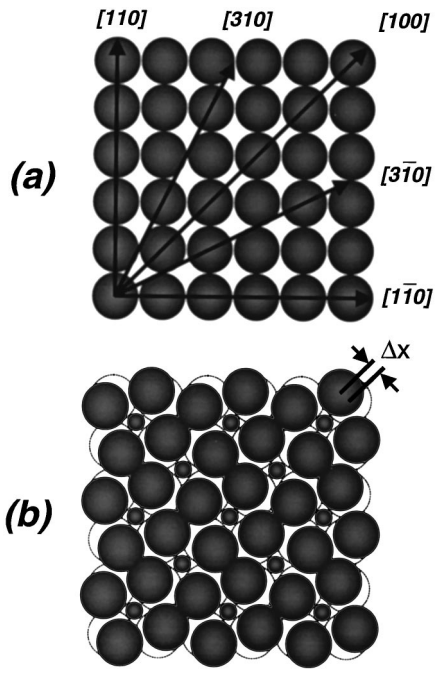


FIG. 1. (a) Structure of a Rh(001) surface. The main crystallographic directions are indicated. (b) Structural model of a Rh(001)-$(2\times2)p4g$-O surface: Large gray spheres indicate the surface rhodium atoms, small gray spheres indicate the adsorbed oxygen atoms. The empty circles show the positions of the rhodium atoms prior to the reconstruction.

¢and annealing at ~1123 K. The temperature was measured by means of a chromel-alumel thermocouple and checked with an infrared pyrometer. The carbon contamination was eliminated by several oxidation and reduction cycles. Surface cleanliness was verified by the absence of O, S, and C in the $He^+$ ion scattering spectra.

Oxygen exposure measurements were carried out by backfilling the chamber with research grade $O_2$ (99.999%) through a leak valve at a pressure of $1\times10^{-8}$ mbar. The doses of oxygen were given in Langmuirs (1 L $=10^{-6}$ Torr s$=1.33\times10^{-4}$ Pa s) as calculated from the uncalibrated ion gauge reading times the time of exposure. As the $(2\times2)p4g$-O structure occurs at saturations (>3.2 L oxygen at room temperature), a constant oxygen pressure ($2\times10^{-9}$ mbar) was maintained during the measurements to replenish oxygen loss to sputtering and to recover the long-range clock rotated ordering. The structure was routinely monitored after the experiments and the sharp $(2\times2)p4g$ LEED pattern was still clearly visible. The surface was cleaned after every incident or azimuthal scan in order to minimize interference from residual gases.

## III. RESULTS

The clean Rh(001) surface exhibited a very sharp $(1\times1)$ LEED pattern with a low background. The $O_2$ dosing on Rh(001) was performed after the sample was cooled down to room temperature. A $p(2\times2)$ LEED pattern was observed after 0.75 L $O_2$ exposure. With increasing $O_2$ dose, sharp $c(2\times2)$ and $(2\times2)p4g$ patterns were obtained at 1.35 and 3.2 L, respectively. The doses of oxygen required for producing the ordered structures are in agreement with previous studies.[3–6] It was suggested[5] that the oxygen coverages on these three surfaces are approximately 0.25, 0.35, and 0.5 ML, respectively, as determined from SPA-LEED. The LEED pattern of the $(2\times2)p4g$ reconstruction is basically just a $(2\times2)$ structure with two glide lines and hence systematic spot extinctions at normal electron beam incidence, while they become visible upon rotation of about 5° around the [001] direction. The glide planes can be related to either a $(2\times2)p4g$ or $(2\times2)p2gg$ reconstruction. STM images of this phase[6] unequivocally show that the symmetry is indeed $(2\times2)p4g$ rather than $(2\times2)p2gg$. Upon heating the surface to temperatures above ~823 K the $(2\times2)p4g$ reconstruction is totally lifted over the whole surface as indicated by the complete loss of the half-ordered beams and the appearance of the sharp $(1\times1)$ pattern of the clean Rh(001) due to oxygen desorption from the surface.

In order to confirm the O adsorption position in the fourfold hollow site for the $(2\times2)p4g$ reconstruction observed in previous LEED patterns[3–5] and STM images,[6] two types of measurements were carried out by detecting negative $O^-$ recoil projectiles under $Ne^+$ ion bombardment. The low-energy recoil process is extremely sensitive to the electronegative O atoms, and the detection of the recoiling species ensures that the adsorption site is probed directly.[13–15] In the first measurement, for azimuthal angle $\phi$ scans at low incident angle $\alpha$ and fixed recoil angle $\Theta$, shadowing features of oxygen shadowed by oxygen and/or oxygen shadowed by rhodium (depending on the O height) along certain directions can be seen. This allows one to identify the O adsorption site. In the second measurement, for incident angle $\alpha$ scans along a fixed high-symmetry azimuth $\phi$, the O-O spacing can be determined by analyzing the shadowing features of oxygen on oxygen and comparison to the results obtained from calculations.

The typical $\phi$ scan of negative $O^-$ recoils for the $(2\times2)p4g$ surface is shown in Fig. 2(a). At a low $\alpha$ angle and along $\phi$ directions corresponding to the alignment of O-O rows, the recoiling centers are inside the shadow cones cast by their nearest neighbors, resulting in low $O^-$ intensity. This is due to the fact that, at grazing incidence, the small impact parameter required for recoiling at $\Theta=60°$ is not accessible. As $\phi$ is scanned, the recoiling centers gradually move out of the shadow cones giving rise to an increase in $O^-$ intensity. The $O^-$ $\phi$ scan exhibits two shadowing dips located at around 0° and 45°, which correspond to the [100] and [110] azimuths. The fact that the shadowing dip at $\phi=0°$ is more pronounced compared to that at $\phi=45°$ reveals the short O interatomic spacing in the [100] azimuth, confirming the O position in the fourfold hollow site. The absence of additional minima induced by rhodium shadowing of oxygen at $\alpha=8°$ is indicative that oxygen is located outside the rhodium shadow cones (i.e., at least 0.5 Å above the surface).

Additional evidence for the O position was obtained from the $\alpha$-scan measurement. Data shown in Fig. 2(b) were collected from the $(2\times2)p4g$ surface along the [100] and [110] azimuths at a recoil angle of $\Theta=60°$, where the $O^-$ peak-area intensities are plotted as a function of $\alpha$. The $O^-$ recoil intensity at small $\alpha$ values is low because each surface atom lies in the shadow cone cast by its preceding neighbor oxygen. The sharp increase observed in the $O^-$ recoil intensity at

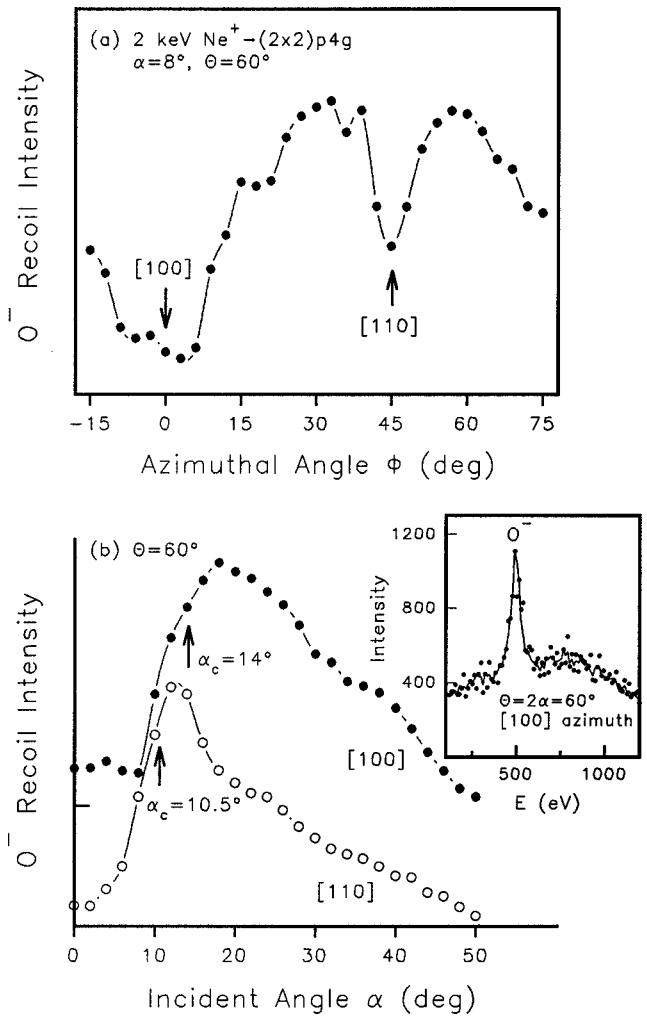


FIG. 2. The $O^-$ recoil intensities obtained from the $(2\times2)p4g$-O surface are plotted (a) as a function of $\phi$ at grazing incidence and (b) as a function of $\alpha$ along the [100] and [110] azimuths at a recoil angle of $\Theta=60°$ using 2 keV $Ne^+$ ions. The inset shows a typical $O^-$ recoil spectrum.

a critical angle $\alpha_c$ corresponds to O atoms moving out of the shadow cone formed by neighboring O atoms. The $\alpha_c$, defined as the $\alpha$ value at 80% $O^-$ peak height, can be related to the O-O spacing through the comparison with calculations.[13]

To determine the O-O spacing, the experimental critical angles $\alpha_c$ for O shadowing of O atoms obtained along the [100] and [110] azimuths have been compared to the values obtained from calculations. The interaction between $Ne^+$ ions and surface O atoms is approximated by the Ziegler-Biersack-Littmark (ZBL) potential. The comparison between the experimental critical angles ($\alpha_c\approx14°$ along the [100] azimuth and $\alpha_c\approx10.5°$ along the [110] azimuth) and the calculated ones ($d_{100}$(O-O)$=3.80$ Å, $\alpha_c=13.9°$ along the [100] azimuth, and $d_{110}$(O-O)$=5.37$ Å, $\alpha_c=10.8°$ along the [110] azimuth) again confirms the O position in the fourfold hollow site within the experimental uncertainty of $\pm0.05$ Å. We also note that the absence of any Rh-O shadowing features at high $\alpha$ angles in the [100] azimuth is due to the fact that oxygen is too high above the surface to be shadowed by rhodium, in agreement with the $O^-$ $\phi$-scan result described above.

On a day to day basis, it was found that the $(2\times2)p4g$ reconstruction was readily produced and very reproducible in such a way that it is a clock rotated rhodium top layer and the four rhodium atoms surrounding the O atom in the fourfold hollow site. The $\phi$ scan in ion scattering is well suited for demonstrating this fact. Figures 3(a) and 3(b) show energy and angle dispersive $\phi$ scans (raw data) at grazing incidence from the clean Rh(001) and $(2\times2)p4g$ surfaces, respectively. The integrated rhodium intensities with linear background subtraction as a function of $\phi$ are shown in Fig. 4(a). The simulated results from the Rh(001) and $(2\times2)p4g$-O surfaces using our laboratory's 3D classical trajectory simulation program[12] are shown in Fig. 4(b), where the rhodium intensity distributions are collected as a function of the rhodium lateral displacement ($\Delta x$) from 0.0 to 0.7 Å at the O height of $\Delta h=0.6$ Å (for details see below).

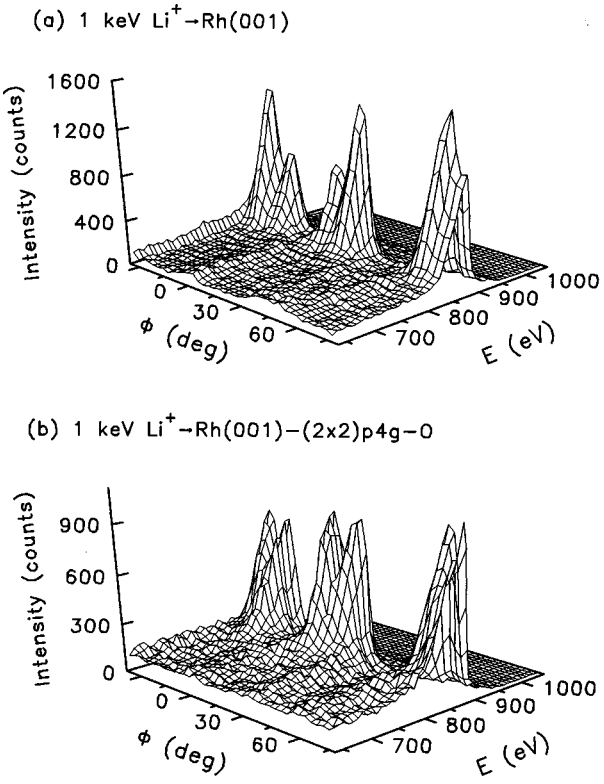


FIG. 3. Experimental ion scattering energy and angle dispersive $\phi$ scans obtained from (a) the clean Rh(001) surface and (b) the $(2\times2)p4g$ surface with 1 keV $Li^+$ ions at $\alpha=10°$ and $\Theta=90°$.

The clean $\phi$ scan exhibits four shadowing minima located at $-18°$, 0°, 18°, and 45°, which correspond to the [310], [100], [310], and [110] azimuthal directions. The deep and wide minima centered at $\phi=0°$ and 45° indicate the short interatomic spacings between surface rhodium atoms in the [100] and [110] azimuths. The shallow and narrow minima at around $\phi=-18°$ and 18° results from the next shortest interatomic spacings along the [310] and [310] azimuths. The displacement of rhodium atoms resulting from the O chemisorption gives rise to different shadowing features in the $\phi$ scan, however it does not produce any new minima. In the case of the Ni(001)-$(2\times2)p4g$-C surface,[9] carbon (coplanar with the Ni first layer) has been shown to have a significant influence on similar ion scattering $\phi$ scans at grazing incidence, giving rise to two additional minima. The

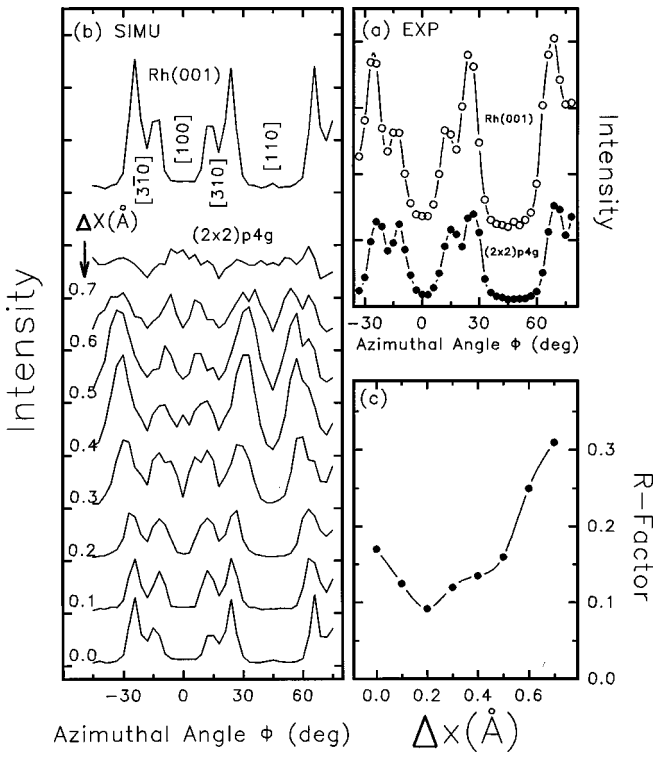


FIG. 4. (a) The experimental (from Fig. 3) and (b) simulated $\phi$ scans obtained from the Rh(001) and $(2\times2)p4g$-O surfaces with 1 keV $Li^+$ ions at $\alpha=10°$ and $\Theta=90°$. The structure used for the simulations was constructed by three layers: the clock rotated rhodium first layer, ideal rhodium second layer, and oxygen overlayer (0.5 ML). Simulated parameters were the ZBL potential, surface rhodium Debye temperature 270 K, oxygen height of $\Delta h = 0.6$ Å, and 160 000 incident projectiles. (c) Plot of the $R$ factor versus the rhodium lateral displacement $\Delta x$ in Å for comparison of the experimental and simulated scans of (a) and (b).

lack of additional minima induced by the O chemisorption can be attributed to the overlayer O position. Since oxygen is located in a high position above the clock rotated rhodium surface (>0.5 Å), it cannot directly shadow individual rhodium atoms but creates an overall decrease in the number of Li projectiles reaching the rhodium surface. The less sharp and narrow shadowing dip at around $\phi=0°$ is a result of several first-layer Rh-Rh interatomic spacings, some of which are double that of the unreconstructed surface causing Rh-Rh alignments not short enough to cast strong shadowing effects along the [100] azimuth. The main shadowing dip along the [110] azimuth at $\phi=45°$ becomes less pronounced, indicating that first-layer Rh-Rh nearest-neighbor atoms are not well aligned. The fact that the shadowing dips at around $\phi=-18°$ and 18° are more clearly resolved compared to those from the clean Rh(001) surface could be interpreted as a result of efficient shadowing caused by the lateral movement of rhodium atoms from their original positions along the [310] and [3$\bar{1}$0] directions. It can be concluded that scattering due to O atoms focusing Li projectiles onto rhodium atoms only makes a small contribution to the overall signal and therefore any features due to O shadowing of rhodium atoms may be masked by features arising from rhodium shadowing of rhodium atoms.

For the $(2\times2)p4g$ surface, the agreement between the experimental and simulated $\phi$ scans was judged on the basis of the reliability $R$ factor as described previously.[12,16] $R$ factors were calculated for comparison of each of the simulated $\phi$ scans with the experimental data. Simulations for the $(2\times2)p4g$ surface were carried out as a function of two parameters: (i) the rhodium lateral displacement ($\Delta x$) from 0.0 to 0.7 Å in steps of 0.1 Å and (ii) the O height ($\Delta h$) above the clock rotated rhodium plane from 0.0 to 1.0 Å. Both the rhodium lateral displacements and the O height above the rhodium surface were varied independently. The result of the $R$-factor analysis is shown in Fig. 4(c), where the $R$ factors are plotted as a function of the displacement $\Delta x$ of rhodium atoms for the simulations from Fig. 4(b). The best fit to the experimental data was achieved with the minimum $R$ factor of $R=0.092$ at $\Delta x=0.2\pm0.1$ Å and $\Delta h=0.6\pm0.1$Å. Repeated measurements involving more than five freshly prepared reconstructed surfaces over several weeks showed that the minimum in $R$ factors was reproducible to within ±15%.

We would like to point out that the structure search was nominally restricted to respect both the glide and mirror symmetries exhibited in the LEED pattern. So far we have only considered the fourfold hollow site. Are the ion scattering data compatible with adsorption in the fourfold bridge site? To test this structure, $R$ factors were also calculated for comparison of each of the simulated $\phi$ scans with the experimental data using the identical procedures described above. The $R$-factor result for the best fit for the fourfold bridge site was 0.11 at $\Delta x=0.2$ Å and $\Delta h=0.6$ Å. Oxygen adsorption in the fourfold bridge site is thus unambiguously ruled out. Furthermore, we can exclude a top site since such a site is unable to produce a glide line symmetry in the LEED pattern. Simple arguments also show that underlayer formation of oxygen is also not compatible with the ion scattering data.

## IV. DISCUSSION

The results of the present investigation have shown that low-energy ion scattering is a highly surface sensitive technique, which is capable of detecting the clock reconstruction and producing quantitative data of the atomic displacement parameters. The $O^-$ negative recoiling $\phi$ and $\alpha$ scans exhibit distinguishing shadowing features that can only be interpreted in terms of the O position in the fourfold hollow site. The lack of any significant Rh-O shadowing features is taken as an indication that oxygen resides above the rhodium substrate. The dominant shadowing features of the $Li^+$ scattering $\phi$ scan are consistent with a $(2\times2)p4g$ phase and a high O position in the fourfold hollow site. Quantitative values for the geometrical parameters were obtained by using a reliability $R$-factor analysis to compare the experimental and simulated $\phi$ scans. For the reconstructed surface, the rhodium atoms rotate in alternating clockwise and anticlockwise directions with the rhodium atoms displaced laterally from their original positions by $0.2\pm0.1$ Å and the O atoms in the fourfold hollow sites at positions $0.6\pm0.1$ Å above the plane of rhodium atoms. These results are in agreement with results from a recent STM study,[6] which has predicted that the degree of rotation and expansion for the Rh(001)-$(2\times2)p4g$-O surface is small, however the geometrical parameters were not previously determined.

In order to understand the driving force for this clock

rotated reconstruction, it is worthwhile to consider the interaction between the adsorbed O and the surface rhodium atoms. It is well established both theoretically and experimentally that adsorption on a surface may induce a considerable negative (compressive) stress.[17] According to the model proposed by Müller, Wuttig, and Ibach[18] for adsorption of C, O, and S on the Ni(001) surface, the strong adsorbate-Ni bond removes charge from the Ni-Ni surface bonds. This leads to finite repulsive forces or stresses between the surface atoms. This model is supported by theoretical calculations based on the effective-medium theory (EMT),[19] which reveal that there exists a considerable contribution to the surface stress from direct adsorbate-adsorbate interactions in these adsorbate-covered Ni(001) systems. The existence of the surface stress induced by the adsorption of C, O, and S on the Ni(001) surface as a function of the adsorbate coverage has recently been verified experimentally by Sander, Linke, and Ibach.[20] For the Ni(001)-C case, the surface stress starts to saturate for C coverage of 0.3 ML, which is correlated with the Ni(001)-$(2\times2)p4g$-C clock reconstruction, in contrast to O and S adsorption, where a parabolalike curve is measured. These observations appear to corroborate the proposal that the development of the surface stress furnishes the driving force for the reconstruction. This may also apply to the Rh(001)-$(2\times2)p4g$-O surface. For the Rh(001)-O system, the $p(2\times2)$ structure is initially formed at a coverage of 0.25 ML. In this phase the O atom is located in the fourfold hollow site with an O height of 0.95 Å and an O-Rh bond length of 2.13 Å.[21] As the coverage increases, the strong adsorbate-substrate interaction leads to the close separation between the O and surface rhodium atoms ($\Delta h = 0.6$ Å with an O-Rh bond length of 1.99 Å determined in this work), thereby resulting in further increase in the surface stress. To relieve the stress, top-layer neighboring rhodium atoms share in a collective way the cost of inducing a $p4g$ clock reconstruction in which the squares of rhodium atoms surrounding the adsorbate O atoms rotate laterally. This produces two perpendicular glide lines along the directions of the missing spots and leads to the experimentally observed systematic extinction of $(0,n+\frac{1}{2})$and $(n+\frac{1}{2},0)$ LEED spots at normal incidence. An alternative explanation is that when the surface is saturated with oxygen at 0.5 ML, stronger, and thus shorter Rh-O bonds are formed. The stronger O-RH interaction must exert a repulsive force on the top layer. Therefore, the surface strain produced by adsorbed O atoms is relieved by directly driving a clock rotation in the top layer. Energetically, this is the cheapest way to lower the surface energy.

It is interesting to compare the Rh(001)-$(2\times2)p4g$-O surface with the Ni(001)-$(2\times2)p4g$-C surface, which has been studied extensively in the past 5 years.[9,22–25] At 0.5 ML coverage, the C atoms penetrate the fourfold hollow sites on Ni(001) by inducing a small radial expansion that is coupled with a large lateral spreading of the four Ni atoms surrounding the C atom. The amount of lateral displacement was determined to be considerable, on the order of 0.5–0.6 Å.[9,22–25] A coplanar geometry allows a stronger adsorbate-metal interaction and in particular a stronger interaction with the second-layer metal atoms. This allows the C atoms to bond directly to Ni atoms in the second layer, giving the necessary energetic justification for such large clock rotations. The driving force behind the reconstruction is the relief of the compressive stress induced by the preference of the small C atoms to be fivefold coordinated. However, the adsorption of oxygen does not reconstruct the Ni(001) surface. This may be a result of the larger atomic radius of oxygen compared to carbon. A recent theoretical calculation based on a tight-binding approximation[26] suggests that for atomic radii larger than a critical value, no substrate reconstruction occurs. For the case of Rh(001) the Rh-Rh distance (2.78 Å) is greater than the Ni-Ni distance (2.49 Å) and the critical radius in this case would be bigger than the O covalent radius. Our ion scattering data show that the O height for the Rh(001)-$(2\times2)p4g$-O phase is significantly larger than that for the Ni(001)-$(2\times2)p4g$-C surface. Therefore, the O clearly induces a much smaller radial expansion on rhodium than observed for the C on Ni. It may be that this much smaller degree of rotation and radial expansion enables the formation of the intermediate $c(2\times2)$ structure.[3–8] Further study with *ab initio* total-energy calculations for establishing the origin of the Rh(001)-$(2\times2)p4g$-O reconstruction is in progress in our surface-science group.

## V. CONCLUSION

We have provided the experimental evidence that for the reconstructed phase, the rhodium atoms rotate in alternating clockwise and anticlockwise directions with the rhodium atoms displaced laterally from their original positions by 0.2 $\pm$0.1 Å and the O atoms in the fourfold hollow sites at positions 0.6$\pm$0.1 Å above the plane of rhodium atoms. Similar to the case of C on Ni(001), the driving force is proposed in which the O adsorbate induces a compressive surface stress which drives the reconstruction of the surface. Experimentally, this Rh(001)- $(2\times2)p4g$-O reconstruction provides well-defined structure which would be an excellent candidate for full dynamical LEED $I$-$V$ studies.

## ACKNOWLEDGMENTS

This work was supported by the Australian Research Grants Scheme. We are also grateful to the University of Newcastle for support with computing time. One of the authors (A.Q.) gratefully acknowledges financial support by the International Atomic Energy Agency (IAEA).

*Author to whom correspondence should be addressed. Present address: Centre for Advanced Materials Technology, Department of Mechanical Engineering, The University of Sydney, NSW 2006, Australia. Fax: +61 2 9351 7060. Electronic address: yshen@mech.eng.usyd.edu.au

†Permanent address: Nuclear Physics Division, Pakistan Institute of Nuclear Science & Technology, P. O. Nilore, Islamabad, Pakistan.

[1] G. A. Somorjai and M. A. Van Hove, Prog. Surf. Sci. **30**, 201 (1989).

[2] D. P. Woodruff, in *The Chemical Physics of Solid Surfaces*, edited by D. A. King and D. P. Woodruff (Elsevier, Amsterdam, 1994), Vol. 7, Chap. 7.

[3] A. Baraldi, V. R. Dhanak, G. Comelli, K. C. Prince, and R. Rosei, Phys. Rev. B **53**, 4073 (1996).

[4] A. Baraldi, L. Gregoratti, G. Comelli, V. R. Dhanak, M. Kiskinova, and R. Rosei, Appl. Surf. Sci. **99**, 1 (1996).
[5] A. Baraldi, V. R. Dhanak, G. Comelli, K. C. Prince, and R. Rosei, Phys. Rev. B **56**, 10 511 (1997).
[6] J. R. Mercer, P. Finetti, F. M. Leibsle, R. McGrath, V. R. Dhanak, A. Baraldi, K. C. Prince, and R. Rosei, Surf. Sci. **352-354**, 173 (1996).
[7] M. Zacchigna, C. Astaldi, K. C. Prince, M. Sastry, C. Comicioli, R. Rosei, C. Quaresima, C. Ottaviani, C. Crotti, A. Antonini, M. Matteucci, and P. Perfetti, Surf. Sci. **347**, 53 (1996).
[8] J. R. Mercer, P. Finetti, M. J. Scantlebury, U. Beierlein, V. R. Dhanak, and R. McGrath, Phys. Rev. B **55**, 10 014 (1997).
[9] J. Ahn, H. Bu, C. Kim, V. Bykov, M. M. Sung, and J. W. Rabalais, J. Phys. Chem. **100**, 9088 (1996).
[10] J. Yao, Y. G. Shen, D. J. O'Connor, and B. V. King, Surf. Sci. **359**, 65 (1996).
[11] Y. G. Shen, A. Bilic, D. J. O'Connor, and B. V. King, Surf. Sci. Lett. **394**, L131 (1997).
[12] Y. G. Shen, J. Yao, D. J. O'Connor, B. V. King, and R. J. MacDonald, Phys. Rev. B **56**, 9894 (1997).
[13] J. W. Rabalais, CRC Crit. Rev. Solid State Mater. Sci. **14**, 319 (1988).
[14] D. J. O'Connor, Surf. Sci. **173**, 593 (1986).
[15] G. Dorenbos, M. Breeman, and D. O. Boema, Phys. Rev. B **47**, 1580 (1993).
[16] M. Copel and T. Gustafsson, Phys. Rev. B **33**, 8110 (1986).
[17] H. Ibach, Surf. Sci. Rep. **29**, 193 (1997).
[18] J. E. Müller, M. Wuttig, and H. Ibach, Phys. Rev. Lett. **56**, 1583 (1986).
[19] K. W. Jacobsen, J. K. Nørskov, and M. J. Puska, Phys. Rev. B **35**, 7423 (1987).
[20] D. Sander, U. Linke, and H. Ibach, Surf. Sci. **272**, 318 (1992).
[21] W. Oed, B. Dotsch, L. Hammer, K. Heinz, and K. Müller, Surf. Sci. **207**, 55 (1988).
[22] J. H. Onuferko, D. P. Woodruff, and S. D. Kevan, Surf. Sci. **87**, 357 (1979).
[23] M. Bader, C. Ocal, B. Hillert, J. Haase, and A. M. Bradshaw, Phys. Rev. B **35**, 5900 (1987).
[24] Y. Gautier, R. Baudoing-Savois, K. Heinz, and H. Landskron, Surf. Sci. **251/252**, 493 (1991).
[25] C. Klink, L. Olesen, F. Besenbacher, I. Stensgaard, and E. Lægsgaard, Phys. Rev. Lett. **71**, 4350 (1993).
[26] S. Reindl, A. A. Aligia, and K. H. Bennemann, Surf. Sci. **206**, 20 (1988).